INTERNATIONAL JOURNAL FOR NUMERICAL METHODS IN FLUIDS
Int. J. Numer. Meth. Fluids 2002; **40**:507–519 (DOI: 10.1002/fld.308)

Novel multigrid orientated solution adaptive time-step approaches

P. G. Tucker*,†

Fluid Dynamics Research Centre, University of Warwick Coventry, CV4 7AL, U.K.

SUMMARY

New performance-improving natural compatabilities between multigrid convergence acceleration and adapted time-step solution procedures are discussed. Echoing the multigrid-coarsened space-steps and interpolations, a novel adaptive temporal 'subcycling' strategy is presented. Tests show, saving storage by basing time-steps on a focused relatively high unsteadiness region, a focused range of variables or multigrid restricted/injected variables can be effective. A novel strategy of advancing comparative solution elements on coarser multigrid levels is found to give time savings. Higher frequency spatial components are accounted for on coarse levels through the multigrid forcing function. Copyright © 2002 John Wiley & Sons, Ltd.

KEY WORDS: adaptive time-steps; multigrid methods; transient flow; cyclic flow; turbulence

1. INTRODUCTION

For many years, when solving general ordinary differential equations (ODEs), temporal type solution adaptive approaches have been used in many scientific fields. Also, when solving the fluid flow equations spatial adaptations have seen significant use [1, 2]. Both approaches can involve the variation of step lengths, discretization orders or a combination of the two.

Generally, whatever numerical resolution approach is used, some form of truncation error estimate is required. The sophistication of this can vary significantly. For example in the spatial adaptation work [3], grid refinement is crudely/indirectly expressed as a function of local variable gradients. More direct approaches compare solutions for example on two grids (i.e. solutions for different step sizes) or schemes of different orders. Multigrid convergence acceleration [4], which uses a hierarchy of grids, with generally a one to two-step coarsening ratio, naturally lends itself to spatial step adaptation [5]. It also has the desirable properties that it can be used to circumvent temporal stability restrictions [6] and coarser levels may

*Correspondence to: P. G. Tucker, Fluid Dynamics, Research Centre, University of Warwick, Coventry CV4 7AL, U.K.
†E-mail: p.g.tucker@warwick.ac.uk

Contract/grant sponsor: EPSRC; contract/grant number: GR/L05600, GR/N05581

Received May 2001
Revised August 2001

more economically model evolving flows—the finer levels being periodically revisited [5]. Therefore, temporal adaptive approaches compatible with multigrid convergence are attractive.

Schonauer *et al.* [7] describe a variable order spatial adaptation for boundary layer flows. Ascher and Petzold [8] give the temporal equivalent to this. In practical cases, due to higher order scheme dispersion, this latter approach is likely to also involve some time-step (Δt) adaptation. For example, when instability is detected Δt can be reduced.

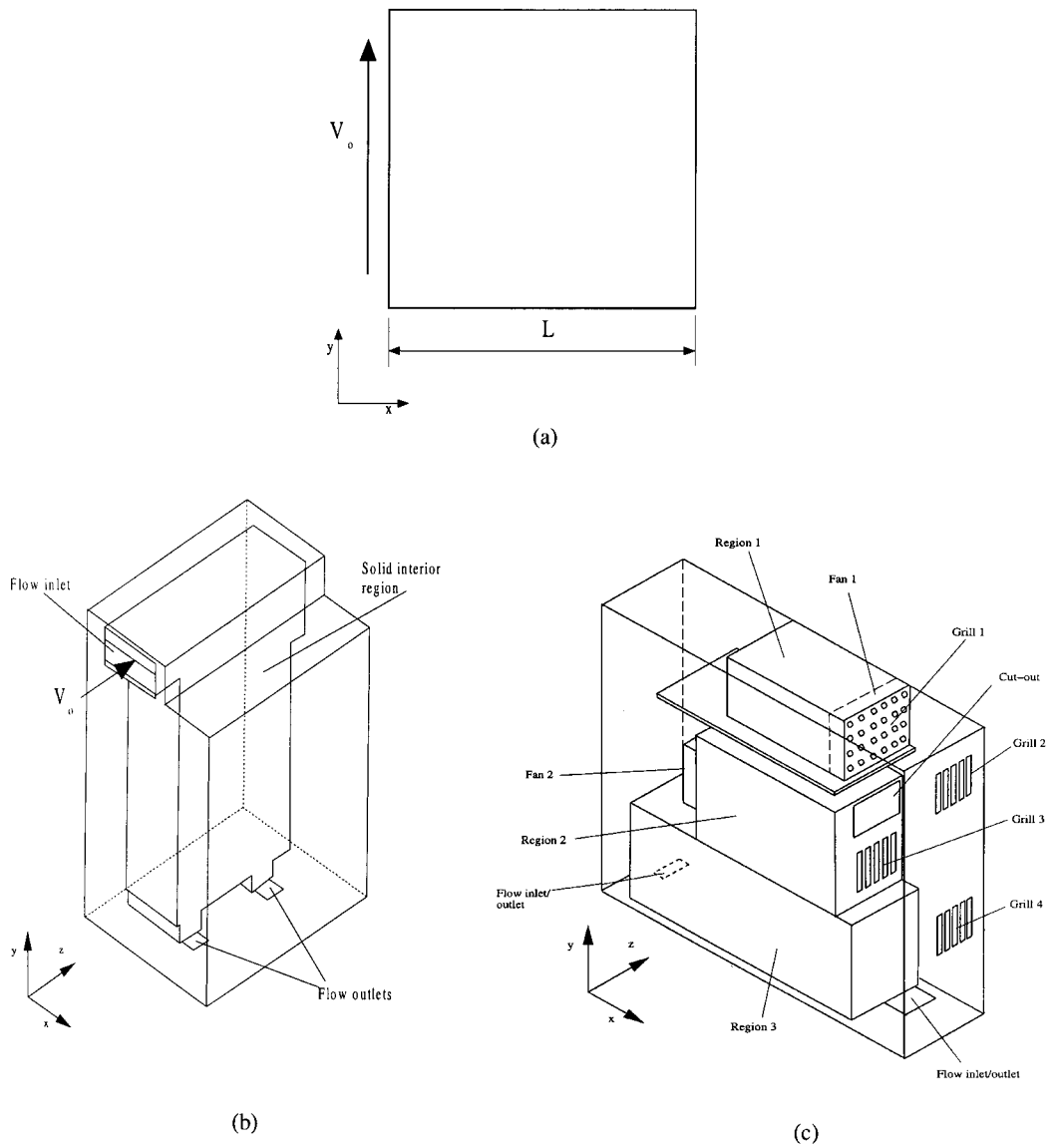

Figure 1. Schematics for Cases (A)–(C): (A) Transient wall driven flow in a square box; (B) Transient flow in a complex system and (C) Cyclic flow in a complex system.

With the exception of the FIDAP finite-element program, in most major commercial codes, little use has been made of adaptive time stepping. Through the method of lines, the discretized flow governing equations can be cast as temporal ODEs. Then, in principle, any standard time adaptive ODE approach [8–10], can be applied to their solution. Possible standard approaches have many similarities to spatial adaptations already more widely used in CFD. The scope here is restricted to adaptive schemes that can most readily be incorporated into commercial codes. Three-dimensional, unsteady, turbulent, non-isothermal industrial flows require significant storage. Since most adaptive time scheme approaches require comparison of two solutions, various storage saving measures are considered. Solution adaptive time-step strategies are tested for the following cases: (A) Transient wall driven flow in a square box; (B) Transient flow in a complex system and (C) Cyclic flow in a complex system. Schematics for Cases (A) and (C) are given in Figure 1.

2. NUMERICAL METHODS

2.1. General solver details

The momentum and turbulence transport equations can be written in the common general form:

$$\rho \frac{\partial \phi}{\partial t} + \rho \nabla \cdot (\mathbf{u}\phi) = \nabla \cdot (\Gamma_\phi \nabla \phi) + S_\phi \tag{1}$$

where ϕ is either a velocity component (u, v or w) or turbulence kinetic energy (k). The source term S_ϕ contains products and gradients of variables, Γ_ϕ a diffusion coefficient and $\mathbf{u}$ a velocity vector. Since the fluid density is constant the corresponding continuity equation can be written as

$$\nabla \cdot \mathbf{u} = 0 \tag{2}$$

The governing equations above (see Reference [11] for their full form) are converted to a discrete form using a finite volume based approach involving SIMPLE and TDMA or a preconditioned conjugate gradient squared method with multigrid convergence [11]. A two-level time (new and old) scheme is produced by making the discretized equation substitution

$$\phi = \frac{(1 + \alpha \Delta t)}{2} \phi^{\text{new}} + \frac{(1 - \alpha \Delta t)}{2} \phi^{\text{old}} \tag{3}$$

The parameter α can be altered to give the following schemes: (I) first-order backwards Euler—$\alpha = \Delta t^{-1}$; (II) Crank-Nicolson—$\alpha = 0$; (III) first-order forwards Euler—$\alpha = -\Delta t^{-1}$; (IV) Damped Crank-Nicolson [12]—$\alpha > 0$ and (V) ADI [13]—α cycled with respect to spatial coordinates taking values of Δt^{-1} or $-\Delta t^{-1}$.

2.2. Time-step adaptation approaches

A crude gradient based method (*GBM*) of Δt adaptation having no direct error estimate is gained by mimicking the spatial approach of Anderson [3]

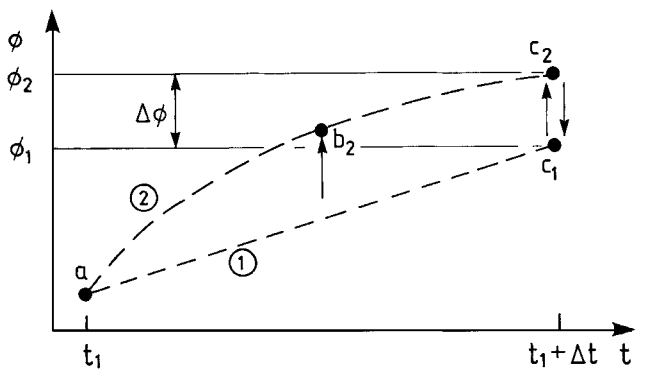

Figure 2. Schematic of general adaptive approach.

$$\Delta t^{\text{new}} = C_t f\left(\frac{1}{1/N_{\phi m}\sum_{i=1}^{N_{\phi m}} |\partial\phi/\partial t|_{\text{ave}}^{\text{old}}}\right) \tag{4}$$

In the above C_t is a scale factor and $N_{\phi m}$ the number of variables considered/solved for (e.g. $u, v, w, k, \ldots$) at a multigrid level m. Since Δt must be spatially constant $|\partial\phi/\partial t|$ should be averaged. Equation (4) has the following deficiencies: Δt is not directly based on the solution error and $|\partial\phi/\partial t|_{\text{ave}}^{\text{old}}$ must be monotonic decreasing (see Case (A) later). More refined and sensible approaches are summarized in Figure 2. This shows two solution elements ((1) and (2)) where $\Delta t \propto \phi_2 - \phi_1$. Solution Element 1 ($a - c_1$) generally has the lower accuracy. Element 2 ($a - b_2 - c_2$) mostly either involves two reduced steps or one higher order step. Alternatively, Elements 1 and 2 can have the same orders and step sizes but use schemes of different natures. From simple Taylor's series manipulation, for a scheme of order $n-1$, the following can be written

$$\Delta t^{\text{new}} = C_t \Delta t^{\text{old}} \left|\frac{\varepsilon}{E^{\text{old}}}\right|^{1/n} \tag{5}$$

where the superscripts 'new' and 'old' now refer to solutions for different step sizes, 'new' being the latest; ε is a pre-set error input value and C_t is now a safety factor. Since Δt must be spatially constant, E^{old}, an estimate of the temporal solution error ($\propto \phi_2 - \phi_1$), needs to be an averaged value. Equation (5) is used here with E^{old} based on: (a) time schemes (I) and (III) (an Altered Scheme (ASc) procedure [14]); (b) time scheme (I) with one full step and two half-steps (an Altered Step ($A\Delta t$) procedure [9]) and (c) time schemes (I) and (II, IV or V) (an Altered Order (An) approach [7, 15]). Ascher and Petzold [8] note approach (b), although easy to implement, can be relatively expensive. Brenan *et al.* [10] show with An approaches action must be taken to deal with instabilities and oscillations. Here the damped scheme (IV) is used to deal with this problem (see Case (C)). Equation (5) is constrained between specified limits so that $\Delta t_{\min} \leqslant \Delta t^{\text{old}}|\varepsilon/E^{\text{old}}|^{1/n} \leqslant \Delta t_{\max}$. For economical evaluation of the averaged E^{old} the following is used

$$E^{\text{old}} = \frac{1}{N_{\phi m}} \sum_{j=1}^{N_{\phi m}} \left[\frac{\int^{R'} |E_{\text{P}\phi}^{\text{old}}|_m \, \mathrm{d}V}{\int^{R'} (|\phi_{\text{P}}^{\text{old}}| + \phi_0)_m \, \mathrm{d}V}\right] \tag{6}$$

where ϕ_0 is a reference scale, V volume, R' the integration domain and $E_{P\phi}^{old} = \phi_{P2} - \phi_{P1}$ where the subscript P indicates the integration effectively involves summation over discrete grid points. Evaluation of (6) generally requires storage of two full solutions. Hence, for a 3D system, with several solution variables it gives a significant storage burden. Therefore, here ϕ is a mostly reduced selected range of variables (with often just $N_{\phi m} = 1$) and $R' \leqslant R$ where R is the full integration region of the fluid. The m subscripts are used to indicate that variables can be restricted (involving producing weighted averages based on surrounding grid point information) or injected (essentially directly transferring information from coincident grid nodes, but here due to grid staggering this involves closest nodes) over R or R' to a coarser grid $m + 1$ (saving storage and a natural part of the multigrid process) and then Equation (6) evaluated.

2.3. Novel subcycling with adaptive time stepping

The subcycling approach [14] applies extrapolated pressures to minor time-steps inside a larger interval (mass conservation is enforced at the larger interval end). A key motivation for this is that evaluating p (pressure) is often relatively expensive. Subcycling and the past practice of using coarser spatial step pressure fields suggests that perhaps p for solution (1) (see Figure 2) could be interpolated to the comparative solution Element (2) without causing significant errors. Specifically solution Element 1 pressures are interpolated/injected to Figure 2 locations b_2 and c_2. Numerous 'subcycling' possibilities exist. Here p from Element (1) is used for (2) with ε small enough to give a negligible conservation error. Hence ϕ_2 is used without mass conservation enforced. Although many engineering turbulence models greatly impact temporal accuracy, this is in an inconsistent fashion. This suggests, like p, certain turbulence parameters could perhaps be subcycled. Since here, a $k - l$ (l is an algebraic turbulence length scale characterization) model is used, this implies a 'subcycling' of k.

2.4. Novel forcing function element adaptation

A novel V cycle based multigrid orientated temporal adaptation approach is illustrated in Figure 3. In this n (subscripted) and ng are used to identify the number of outer iterations at a particular grid level and the maximum number of levels, respectively. The coarsest level corresponds to $m = \text{ng}$. The cycle starts at the finest grid ($m = 1$) continuing to the coarsest and then returning to $m = 1$ describing the left-hand side of the Figure 3 V shape (temporal solution Element 1 of Figure 2). This solution element V cycle is repeated for n iterations corresponding to Element 1 time-step convergence. Brandt [5] proposed that for evolving flows finest grid levels ($m = 1$) can just be periodically revisited, most time advancement effort being more economically focused on the coarser levels ($m > 1$). The finer level information is sensed on coarse grids through a *forcing function* [5]. This function is an additional discretized equation source term that ensures coarser grid solutions are an exact (but, through the restriction operators, in a weighted average sense) of the fine grid ($m = 1$) solution. This non-adaptive solution strategy suggests that the first adaptive solution Element (1) could be used to generate a forcing function for Element (2), the latter just being advanced on computationally cheaper $m > 1$ grids. The Figure 3 schematic is directly applicable to the An (An_m) and ASc (ASc_m) approaches. For the $A\Delta t$ approach ($A\Delta t_m$), here, both half-steps are advanced at $m = 2$, adding another single iteration stage with forcing function assembly to Figure 3. Other possible arrangements are not explored here. Also, no ASc_m implementation is made.

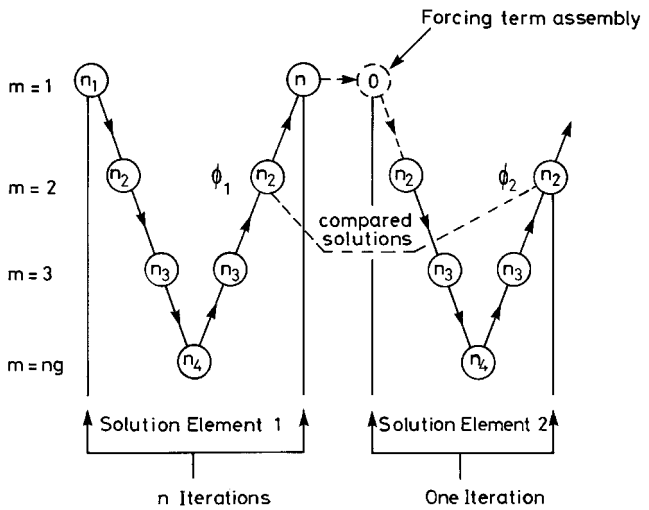

Figure 3. Novel V cycle based multigrid adaptation approach.

This is because generating a forcing function from the stable backwards Euler element, for use in the forwards Euler would, except for extremely dense grids, yield little computational benefit. The explicit component is already extremely cheap.

3. DISCUSSION OF RESULTS

3.1. Solution set-up and parameter details

For all the time-step adaptive solutions, because of the significant Δt variations, to avoid divergence under-relaxation is found necessary. This is not needed for all fixed step cases. Generally, no effort is made here to find optimal relaxation parameter (α) values and what are felt to be conservative levels are used. Under-relaxation is incorporated directly through the coefficients of the discretized equations. For all cases $\varepsilon = 0.1\%$, $\rho = 1.3\,\mathrm{kg/m^3}$, $\mu = 1.83 \times 10^{-5}\,\mathrm{kg/ms}$. With the simpler Case (A) geometry/flow $C_t = 0.9$ in Equation (5). For all other cases $C_t = 0.45$. Nominal set up parameters for adaptive scheme solutions are given in Table I. The parameters n_p and y^+_ave represent the number of pressure sweeps (sweeps of the TDMA solver for corrections to p) and average first off-wall grid node position in wall units, respectively. The velocity reference scale V_0 is used in the evaluation of percentage solution errors. Tabulated Δt values correspond to those required for sensibly time step independent solutions. Convergence is based on either normalized residuals or the maximum root mean square ($\mathrm{rms}_{\phi,\max}$) for a particular variable where

$$\mathrm{rms}_\phi = \sqrt{\frac{\sum_R (\phi^{\mathrm{new}} - \phi^{\mathrm{old}})^2}{\sum_R (\phi^{\mathrm{new}})^2}} \tag{7}$$

The Equation (7) superscripts are used in an iterative sense and the summations applied over all $m = 1$ grid points. At solid walls, for velocities, the usual no-slip and impermeability

Table I. Nominal parameter values for Cases (A)–(C).

Case	A	B	C
Dimensionality	2D	2D	3D
Grid density	$33 \times 33 - 121 \times 121$ (x, y)	101×101 (x, y)	$101 \times 89 \times 45$ (x, y, z)
Adaptation Variables	u and v and just v	u and v and just v	u
Δt (s)	0.001	0.001	0.001
$\Delta t_{\min}$ (s)	0	0.0001	0.001
$\Delta t_{\max}$ (s)	∞	0.5	NA
C_t	0.9	0.45	0.45
$\alpha_{u,v,w,k}$	0.3	0.5	0.4
α_p	0.7	1	0.7
ng	4	1	1
n_p	6	16	6
y^+_{ave}	NA	—	15
V_0 (m/s)	1.52×10^{-4}	3.8	4.5
v_0 (m/s)	1×10^{-10}	3.8	1×10^{-10}
$\text{rms}_{\phi,\max}$	2.5×10^{-5}	1×10^{-4}	NA
Residual error (%)	NA	NA	0.5

conditions are applied. At open boundaries, p is fixed and generally the gradients of other variables are set to zero in a second order fashion.

3.2. *Transient wall driven flow—case (A)*

The Case (A) geometry is shown in Figure 1a. When $t > 0$, $Re = 400$. The steady flow is a popular benchmark for which uniform grids [16] are most effective. The uniform Figure 4 grid, with the multigrid embedded [2] region near the moving wall is sufficient for sensible steady flow grid independence. Figure 5 shows contours of $\partial v/\partial t$ at $t = 0.25$, 0.5, 1 and 1.25 s. It is clear that, like the spatial gradients, the key temporal gradients occur around $X < 0.5$ (X is the dimensionless x co-ordinate such that $1 \geqslant X \geqslant 0$). This information is exploited in the Δt adaptation strategy.

Figure 6 gives a linear-log plot for the cell area weighted average of $\partial v/\partial t$ (over $R' = R$) against t. Away from the initial transient, the $\partial v/\partial t$ variation is approximately linear suggesting the case is amenable to the crude GBM (Note, $t > 40$s oscillations are due to $\partial v/\partial t$ approaching zero and hence machine round-off error). However, despite significant efforts, no satisfactory relationship, between temporal gradients and Δt^{new} could be found. Therefore this approach was abandoned. It was concluded for more complex flows, a relationship between $|\partial\phi/\partial t|_{\text{ave}}$ and Δt would generally be too time consuming to find.

Table II gives: nominal percentage savings in computing time (t_s) (relative to a $\Delta t = 0.03$ s solution, giving a highly conservative estimate of adaptive Δt performance), the per centage of time-steps where $E'_{\text{ave}} > \varepsilon$ (hence needing to be recomputed) and E'_{ave} (the true average solution error). Percentage errors are based on the driven wall velocity V_0. Also, tabulated is E'_{ave} for $t < 5$ s with E^{old} evaluated for both $R' \approx R$ (column 5) and $X \leqslant 0.5$ (i.e. $R'/R < 1$) as shown in column 6. Errors are further considered for $R'/R < 1$ when Equation (6) is calculated at $m = 2$ with storage saving *injection* (column 7) and a 6 point restriction (column 8).

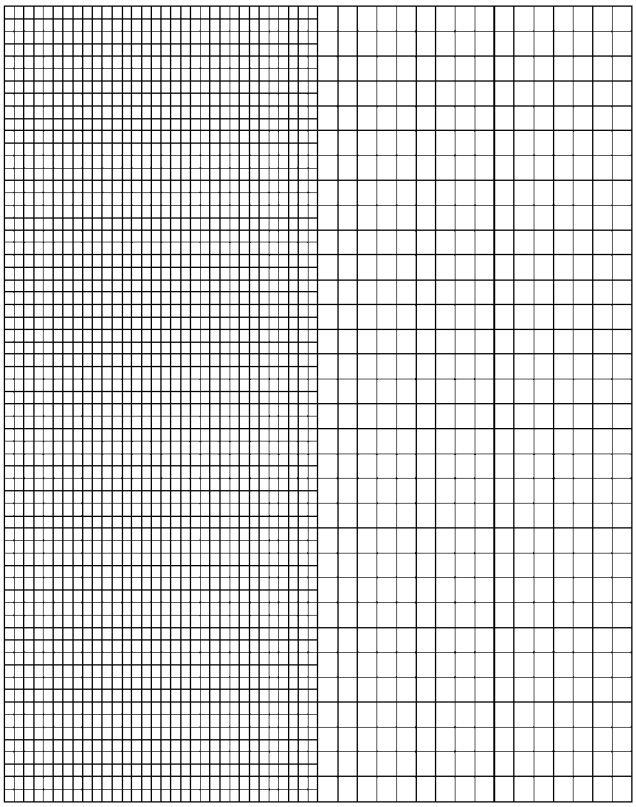

Figure 4. Embedded grid.

Results show the storage reduction of evaluating E^{old} over R' has slightly improved accuracy. As might be expected, applying Equation (6) with $m=2$ and injection reduces accuracy. Surprisingly, full restriction, that absorbs more information from the finest grid level, with (6) generally reduces accuracy further. Nonetheless for most engineering applications the accuracy is more than acceptable. Importantly, use of just v or both u and v in (6) has little performance influence. Considering its computational limitations (see Reference [8]) the $A\Delta t$ scheme performance is surprisingly good. Table II suggests p 'subcycling' (p_sc) is promising. Perhaps the An(p_sc) method shows both accuracy and speed gains because either spurious wiggles or minor convergence error components in the higher order solution are suppressed. This probably arises from using the more robust lower order pressure field solution component. It is worth noting here that with the significant range of time-steps occurring through an adaptive solution, discretized equation diagonal dominance can vary dramatically. Preliminary tests using a conjugate gradient solver which is more robust with respect to diagonal dominance shows smoother and more promising general $t \to \infty$ behaviour. Pleasingly, unlike the $A\Delta t_m$, the An_m approach does not appear to significantly reduce accuracy whilst producing around a 20% t_s improvement.

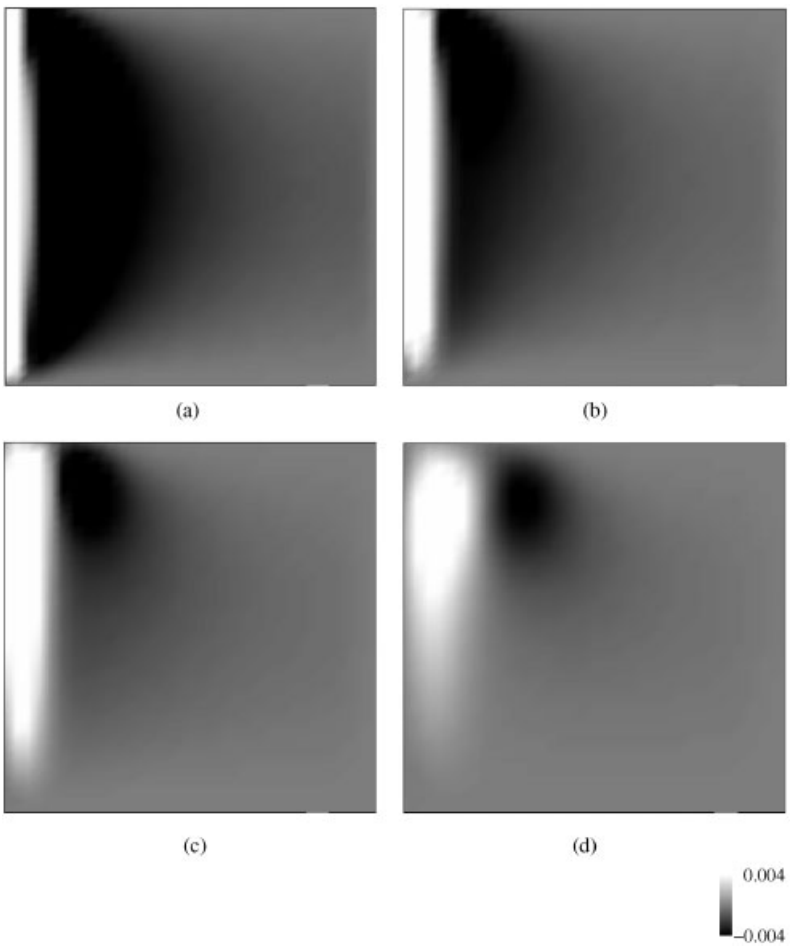

Figure 5. Case (A) contours of $\partial v/\partial t$ (m/s^2) at: (a) $t = 0.25$ s, (b) $t = 0.5$ s, (c) $t = 1$ s and (d) $t = 1.25$ s.

3.3. *Transient flow in a complex system—Case B*

Figure 1(b) gives a schematic of the industrially motivated Case (B) geometry. Tucker and Pan [17] present full case details. This simulation is especially computationally expensive. Therefore, 2D high Reynolds number $k-l$ [11] predictions are used, the inlet condition being adjusted to make the 2D temporal response approximately match the 3D response. The 2D-solution plane incorporates the single flow inlet and two flow outlets. Basing temporal error estimates (Equation (6)) on just u (saving storage) or both u and v makes little difference to results.

Table III summarizes adaptive scheme performances for $t < 1.6$ s. Again, the ASc scheme shows best performance. However, even this is 1.5% *slower* (identified using the minus signs in the table) than the $\Delta t = 0.01$ s solution. Nonetheless, the ASc E'_{ave} is 15% less than the $\Delta t = 0.01$ s and so this result should not be considered as completely negative. Performances

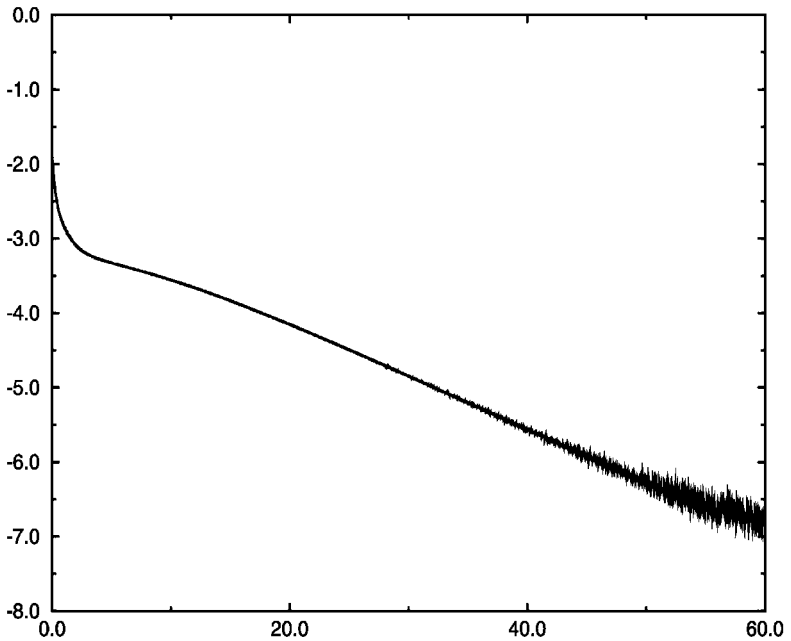

Figure 6. Case (A) time history.

Table II. Case (A) adaptive scheme performances.

Scheme	t_s (%) ($t<60$ s)	% Δt Fails ($t<60$ s)	% E'_{ave} ($t<60$ s)	% E'_{ave}, $t<5$ s			
				Full region R	Half region R'		
					Standard	Injection	Restriction
GBM	0	NA	NA	NA	NA	NA	NA
An	31	3.2	0.019	0.030	0.029	0.032	0.032
An(ADI)	31	0.07	0.017	0.018	—	—	—
ASc	57	0.80	0.055	0.023	0.022	0.024	—
$A\Delta t$	56	0	0.062	0.024	0.023	0.025	0.028
An(p_sc)	51	—	0.009	—	—	—	—
$A\Delta t$(p_sc)	73	—	0.077	—	—	—	—
An_m	50	0	0.02	—	—	—	—
$A\Delta t_m$	20	0	0.18	—	—	—	—

for all the other standard approaches seem especially disappointing. Therefore, 'subcycling' is again tried. Relative to the standard schemes, the table shows clear t_s improvements with just modest E'_{ave} *increases*. The latter increases make these 'subcycling' results slightly inconclusive. However, reminiscent of Case (A), when comparing the An(p_sc) and An(p,k_sc), results 'subcycling' has given an accuracy improvement. This suggests it has the inherent positive trait of enhancing stability. Storage saving injection and restriction seems to have

Table III. Case (B) adaptive scheme performances.

Scheme	t_s (%)	% Δt Fails	% E'_{ave}		
			Standard	Injection	Restriction
$\Delta t = 0.01$ s	NA	NA	0.18	—	—
An	−38	0	0.12	0.12	0.12
ASc	−1.5	0	0.15	0.15	0.15
$A\Delta t$	−56	0	0.12	0.12	0.12
An(p_sc)	−28	—	0.16	—	—
An(p, k_sc)	−23	—	0.15	—	—
$A\Delta t$(p_sc)	−40	—	0.21	—	—
$A\Delta t$(p, k_sc)	−39	—	0.22	—	—

Table IV. Case (C) adaptive scheme performances.

Scheme	t_s (%)	%Δt fails	% E'_{ave} over one unsteadiness cycle		
			Full region	R' region	
				Standard approach	Injection
An	86	0	0.152	0.140	0.141
ASc	61	0	0.065	0.055	0.058
$A\Delta t$	87	0	0.240	0.160	0.163

negligible affect on accuracy. One observed difficulty, that explains most of the poorer Case (B) performance, is that initial transient severity causes numerical instabilities. These result in adaptive schemes predicting extremely small steps. Usefully, the instability gives an in-built conservativeness.

3.4. *Cyclic flow in a complex system—Case (C)*

Figure 1c gives the Case (C) geometry. Tucker [11] presents full case details. The flow is driven by fans represented by quadratic momentum sources. Quadratic sink terms model grills. The $k - l$ model is again used. For the multiple Case (C) quadratic source terms [18] and Neumann boundary conditions [19] Scheme (II) stability is not guaranteed. Therefore, to control error growth, instead method (IV) is used with $\alpha = 2.5$. A further measure, motivated by Scheme (II) concerns is limiting time-steps so that Courant numbers are below 5. The temporal error estimate (Equation (6)) is based on the key variable of interest here, which is the fluid x velocity component. Due to computational expense, the strategies tested are limited. Therefore, for example, no tests involving saving storage by using multilevel restriction operators are made. Instead just injection is tried. Analysis shows most unsteadiness is focused around $Y > 0.75$ (the top quarter of the system). Performances of different schemes, for one unsteadiness cycle, are summarized in Table IV.

The table shows all schemes give solutions close to the specified 0.1% error and significant (on average 78%) time savings (Note, the comparative solution error time-step for this case

was to a large extent based on best computational convergence grounds). For this case, the ASc approach appears least efficient. Although the An method looks most effective, as noted in the foregoing discussion, rather case specific stability measures are required. On these grounds, for this case, the stable $A\Delta t$ approach probably should be considered best. Table IV indicates evaluating (6) over R' increases accuracy and reduces storage. Pleasingly, novel storage saving injection just gives minor (on average 0.0025%) error increases.

4. CONCLUSIONS

Novel, performance-improving natural compatabilities between multigrid convergence and adapted time-step (Δt) solution procedures have been illustrated. These compatabilities can yield both storage and time-savings (t_s). Echoing the multigrid coarsened space steps and interpolations, novel temporal 'subcycling' strategies are also considered. Out of the standard ASc, $A\Delta t$ and An schemes none is clearly superior. The $A\Delta t$ stability seems to balance its extra cost. The 'subcycling' approximation generally improves t_s but can increase the solution error. For all cases, where storage is saved by basing Δt on regions of greatest unsteadiness accuracy improvements are found. Also, the multigrid convergence compatible, injection storage saving introduces negligible solution error. However, surprisingly, full multigrid restriction, which absorbs more fine grid information, produces a slightly higher error (nonetheless, relative to the overall solution error the increase is minor). Tests show that, saving storage by basing time-steps on a restricted range of variables can also be effective. For the An approach, advancing the subsequent comparative solution element on coarser grid levels is found effective (19% additional time saving). Higher frequency spatial components are accounted for on coarse levels through the multigrid convergence forcing function.

For certain cases, the use of Δt clipping is found important—especially to prevent excessively small steps. These can instead be limited by the choice of appropriate reference values. Whether clipping or reference values are used partly depends on data availability. Cases reveal that solver robustness is a key issue. Time-steps and hence diagonal dominance can vary dramatically over a solution.

With increasing solver robustness and affordable computer storage, the use of adaptive time-stepping is likely to increase. For future work, conjugate gradient type solvers, that are less sensitive to diagonal dominance, might be worth testing further. Also, with parallel architecture machines, the two comparative solution elements could be completed concurrently. This is likely to yield dramatic performance gains and so is worthy of future study. Generally, the first solution component should be a good guess to the second. Then a Newton type solver would be highly efficient. Therefore, testing the use of a Newton type solver for the second solution element also appears worthwhile future work.

ACKNOWLEDGEMENTS

The present work relates to EPSRC grants GR/L05600 and GR/N05581. The latter award is for the study of unsteady flows in complex geometries. This funding is gratefully acknowledged.

REFERENCES

1. Davis RL, Dannenhoffer JF. Three-dimensional adaptive grid-embedding Euler technique. *AIAA Journal* 1994; **32**(6):1167–1174.

2. Thompson MC, Ferziger JH. A multigrid adaptive method for incompressible flows. *Journal of Computational Physics* 1989; **82**:94–121.
3. Anderson JD. *Computational Fluid Dynamics: The Basics with Applications*. McGraw-Hill Inc.: New York, 1995.
4. Brandt A. Multi-level adaptive solutions to boundary-value problems. *Mathematics of Computation* 1977; **31**(138):333–390.
5. Brandt A. Multilevel adaptive computations in fluid dynamics. *AIAA Journal* 1980; **18**(10):1165–1172.
6. Dimitriadis KP, Leschziner MA. Multilevel convergence acceleration for viscous and turbulent transonic flows computed with cell-vertex method. In *Proceedings of the 4th Copper Mountain Conference on Multigrid Methods*, Colorado 1989; 1–15.
7. Schonauer W, Glotz G, Raith K. The solution of the laminar boundary layer equations by a variable order self adaptive difference method. In *Recent Advances in Numerical Methods in Fluids*, Taylor C, Morgan K (eds), vol. 1, Pineridge Press Ltd, Swansea, UK, 1980; 81–118.
8. Ascher UM, Petzold LR. *Computer Methods for Ordinary Differential Equations and Differential Algebraic Equations.* SIAM: Philadelphia, PA, 1998.
9. Press WH, Flannery BP, Teukolsky SA, Vetterling WT. *Numerical Recipes*: *The Art of Scientific Computing*. University of Cambridge Press: Cambridge, 1988.
10. Brenan KE, Campbell SL, Petzold LR. *Numerical Solution of Initial Value Problems in Differential Algebraic Equations*. SIAM: Philadelphia, PA, 1996.
11. Tucker PG. Prediction of turbulent oscillatory flows in complex systems. *International Journal for Numerical Methods in Fluids* 2000; **33**:869–895.
12. Hujeirat A, Rannacher R. A method for computing compressible, highly stratified flows in astrophysics based on operator splitting. *International Journal for Numerical Methods in Fluids* 1998; **28**:1–22.
13. Peaceman DW, Rachford HH. The numerical solution of parabolic end elliptic differential equations. *SIAM Journal* 1955; **3**:28–41.
14. Gresho PM, Chan ST, Lee RL, Upson CD. A modified finite element method for solving the time-dependent, incompressible Navier–Stokes equations. Part 1: theory. *International Journal for Numerical Methods in Fluids* 1984; **4**:557–598.
15. Skelboe S. The control of order and steplength for backward differentiation methods. *BIT* 1977; **17**:91–107.
16. De Vahl Davies G, Jones IP. Natural convection in a square cavity: a comparison exercise. *International Journal for Numerical Methods in Fluids* 1983; **3**:227–248.
17. Tucker PG, Pan Z. Computation of transient turbulent isothermal flow with a plane jet. In *Proceedings of the ASME Heat Transfer Divisions Winter Meeting*, Witte LC (ed.), vol. 364, 1999; 253–260.
18. Wilcox DC. *Turbulence Modelling for CFD*. DCW Industries: Berlin, 1998.
19. Fletcher CAJ. *Computational Techniques for Fluid Dynamics*: *Fundamental and General Techniques*, vol. 1. Springer: Berlin, 1997.

